

The Debris Disk Candidates: Eleven $24\mu\text{m}$ excess stars in *Spitzer* SWIRE Fields

Hong. Wu¹, Chao-Jian Wu², Chen Cao^{3,4}, Sebastian Wolf⁵ and Jing-Yao Hu¹

¹ Key Laboratory of Optical Astronomy, National Astronomical Observatories, Chinese Academy of Sciences, Beijing 100012, P.R. China; *hwu@bao.ac.cn*

² Department of Astronomy, Beijing Normal University, Beijing, 100875, P.R. China

³ Institute of Space Science and Physics, Shandong University at Weihai, Weihai, Handong 264209, P.R. China

⁴ Shandong Provincial Key Laboratory of Optical Astronomy & Solar-Terrestrial Environment, Weihai, Shandong, 264209, P.R. China

⁵ Max Planck Institute for Astronomy, Königstuhl 17, 69117 Heidelberg, Germany

Abstract We present the optical to mid-infrared SEDs of 11 debris disk candidates from *Spitzer* SWIRE fields. All these candidates are selected from SWIRE $24\mu\text{m}$ sources matched with both the SDSS star catalog and the 2MASS point source catalog. They show an excess in the mid-infrared at $24\mu\text{m}$ ($K_S-[24]_{Vega} \geq 0.44$) indicating the presence of a circumstellar dust disk. The observed optical spectra show that they are all late type main-sequence stars covering the spectral types of FGKM. Their fractional luminosities are well above 5×10^{-5} , even up to the high fractional luminosity of 1×10^{-3} . The high galactic latitudes of SWIRE fields indicate that most of these candidates could belong to the oldest stars in the thick disk. Our results indicate that the high fractional luminosity debris disks could exist in the old solar-like star systems, though they are now still quite rare. Their discoveries at high-galactic latitudes will also provide us an excellent opportunity to the further studies of properties and evolution of the debris disk in the ISM poor environments.

Key words: infrared: stars – planetary systems: protoplanetary disks – stars: formation

1 INTRODUCTION

One of the most notable achievement of the *InfraRed Astronomical Satellite* (IRAS) is the discovery of dusty circumstellar disks (Zuckerman, 2001). An example is Vega, which shows a large infrared excess from a main-sequence star (Aumann et al., 1984). This provided the direct evidence to the existence of a debris disk firstly. The scattered light from several nearby debris disks has been analyzed by use of the

disks left over from star formation (Hollenbach et al., 2000; Wyatt & Dent, 2002; Gorlova et al., 2004). The study of debris disks is crucial to understand the formation and existence of planets (Bryden et al., 2009) and smaller objects, such as comets and asteroids (Zuckerman, 2001).

Limited by the sensitivity of IRAS, most of the debris disk discovered were for nearby stars much younger than the sun (Metchev et al., 2004; Bryden et al., 2006), since they are likely to be at a transition stage with a higher frequency to possess a disk with a plenty of dust (Zuckerman & Song, 2004; Bryden et al., 2006), and their luminosities are high enough to heat a debris disk to an IRAS-detectable level (Krist et al., 2005). With the higher sensitivity, better resolution and the more extended wavelength (Jourdain de Muizon et al., 1999), the *Infrared Space Observatory (ISO)* has expanded our capability of searching for circumstellar dust (Spangler et al., 2001) to the modest infrared excess among the older stars (Decin et al., 2000, 2003; Habing et al., 2001).

With the launch of the *Spitzer* Space Telescope (Werner et al., 2004), a new level of sensitivity and spatial resolution is provided to the studies of debris disks in the infrared (Su et al., 2005). It provides the potential to identify and investigate the debris systems that were not detectable with previous observatories (Kim et al., 2005). It also extends the search for debris disks to larger distances (Bryden et al., 2006). Several *Spitzer* programs have focused on this field, including the Cores to Disks (Evans et al., 2003, C2D), Formation and Evolution of Planetary Systems (Meyer et al., 2004, FEPS), the Galactic Legacy Infrared Mid-plane Survey Extraordinaire (Benjamin et al., 2003, GLIMPSE), and the Survey of Solar-Type Stars (Beichman et al., 2005, SSS). However, most of these programs are designed for the search of the infrared excess in either nearby known planetary systems or the debris systems at regions, where interstellar material is rich, such as the low galactic latitude regions and the molecular clouds. While, at high Galactic latitudes, there are also some wide-area surveys with the Multiband Imaging Photometer for *Spitzer* (Rieke et al., 2004, MIPS), such as the NOAO Deep Wide-Field Survey (Jannuzi & Dey, 1999; Houck et al., 2005; Brand et al., 2006), the *Spitzer* Wide-area Infrared Extragalactic Survey (Lonsdale et al., 2003, SWIRE), and the *Spitzer* extragalactic First Look Survey (Fadda et al., 2006, xFLS), which provide us more star candidates with infrared excesses (Hovhannisyan et al., 2009).

The *Spitzer* SWIRE were observed in the four mid-infrared IRAC bands (3.6, 4.5, 5.8, 8.0 μm) (Fazio et al., 2004) and the three mid-to-far infrared MIPS bands (24, 70, 160 μm) (Rieke et al., 2004). Being designed for extragalactic surveys, all the six SWIRE fields are at high galactic latitudes and cover about 50 sq. degree. The wide field and high sensitivity provide us an opportunity to search for the new faint debris disk candidates even the planets (Bryden et al., 2009) in the thick disk or even in the halo. Contrary to the other *Spitzer* programs mentioned above, which focus on the younger or nearby systems, the debris disk candidates selected from SWIRE fields are much farther in distance from 300 to 2,000 pc compared with those which have a distance from 10 to 150 pc in FEPS, and also much older in age of about 10 Gyr belonging to the oldest systems. Generally, the star that is older than 10 Myr can be regarded as a candidate with debris disk (Gorlova et al., 2006). This sample will help us to explore the formation of planetary

In this paper, we first describe the optical to infrared observations, data reduction and candidate selection in Section 2. In Section 3, we give the infrared properties of these $24\mu\text{m}$ excess stars, their spectral energy distributions (SEDs). The discussions and summary are presented in Section 4 and 5.

2 DATA, OBSERVATIONS AND CANDIDATE SELECTION

2.1 *Spitzer* Mid-Infrared Data and Data Reductions

The $24\mu\text{m}$ excess stars are from ELAIS-N1, ELAIS-N2, Lockman Hole fields of the SWIRE fields. The common regions of observations between the IRAC and MIPS for ELAIS-N1, ELAIS-N2, and Lockman Hole fields are about 8, 4, and 11 sq. degree (Surace et al., 2005). The BCD (Basic Calibrated Data) images of the IRAC four bands were obtained from *Spitzer* Sciences Center (SSC), which include flat-field corrections, dark subtraction, linearity and flux calibrations (Fazio et al., 2004). The IRAC images were mosaiced from the BCD images after pointing refinement, distortion correction and cosmic-ray removal with the final pixel scale of $0.6''$ as described by Huang et al. (2004) and Wu et al. (2005); Whilst the MIPS $24\mu\text{m}$ images were mosaiced in the similar way with the final pixel scale of $1.225''$ (Wen et al., 2007; Cao & Wu, 2007). Matching the sources detected by SExtractor (Bertin & Arnouts, 1996) in the five bands (IRAC four bands and MIPS $24\mu\text{m}$ band) with the 2MASS sources, we obtained the astrometric uncertainties of less than $0.5''$.

The mid-infrared photometries were obtained by SExtractor with an aperture of $3''$ for the IRAC four bands and $10.0''$ for the MIPS $24\mu\text{m}$ band. All these magnitudes are in AB magnitude system (Oke & Gunn, 1983). All the magnitudes of four IRAC bands were corrected the aperture of $24''$. Comparing with the model colors of IRAC magnitudes and 2MASS K_S magnitude (Cutri et al., 2003) for the 2MASS stars with $J-K_S \leq 0.3$ as (Lacy et al., 2005) did for sources in *Spitzer* xFLS field, the small additional corrections were made for all the four IRAC bands. And these give us the calibration errors in the four IRAC bands better than 0.08 mag. As for $24\mu\text{m}$, the magnitudes were first corrected to the aperture of $30''$. Then an additional correction was also performed according to Surace et al. (2005). The calibration accuracy of $24\mu\text{m}$ is better than 10% (Rieke et al., 2004). The 5σ flux in the IRAC four bands and MIPS $24\mu\text{m}$ band are about 5, 8, 43, 43 and $200 \mu\text{Jy}$ respectively.

2.2 Optical and Near-IR Photometries

The ELAIS-N1, Lockman Hole and ELAIS-N2 fields are completely or partly covered by the Sloan Digital Sky Survey (Stoughton et al., 2002, SDSS) and the total overlap regions used in this work is about 15 sq. degree. All the *Spitzer* sources were matched with the SDSS point sources from "Star" catalog of Data Release 4 (Adelman-McCarthy et al., 2006) with a radius of $3.0''$. The PSF magnitudes of u, g, r, i, z bands were adopted in this work. The near-infrared magnitudes were from the 2MASS point source catalog (Cutri et al., 2003). The default J, H, K_S band magnitudes were adopted.

2.3 Candidate Selection

Gorlova et al. (2004) studied the $24\mu\text{m}$ emission of the M47 stars, and found that the majority of them

they defined the $24\mu\text{m}$ excess stars as those 3σ redder than the mean value, that is, $K_S-[24]_{Vega} \geq 0.44$. We adopted their selection criterion to select $24\mu\text{m}$ excess stars. $[24]_{Vega}=[24]_{AB}-6.74$ was used to transform the AB magnitudes in the $24\mu\text{m}$ band to the Vega magnitudes. To obtain the optical spectra, we only selected stars with r magnitudes less than 17.5. We also removed the objects with fuzzy features, whose $24\mu\text{m}$ emission could come from the background galaxies. Finally, we selected 11 $24\mu\text{m}$ excess candidates. Figure 5 shows the locations of all the candidates in the color-color diagram and the selection criterion is also plotted as a vertical dotted line. Their names and the optical to infrared magnitudes of the candidates are listed in Table 1. Since there are problems in the r magnitude of the star J163754.26+405259.1 and the g, r, i magnitudes of the star J163948.68+413711.0, we did not include these measurement in our subsequence analysis. From Table 1, we can see that except J104508.69+592830.5, all these candidates have $K_S-[24]_{Vega}$ value above 1, indicating strong $24\mu\text{m}$ excess. The optical r -band, IRAC $3.6\mu\text{m}$, $8.0\mu\text{m}$ and MIPS $24\mu\text{m}$ images are shown in Figure 1. The central circle in each image indicates the optical position of each star with a radius of $1.5''$. It can be seen that all positions in the four bands are consistent.

2.4 Optical Spectroscopy

The optical spectra of 11 debris disk candidates stars were obtained with the 2.16m telescope at Xinglong, NAOC (National Astronomical Observatories, Chinese Academy of Sciences) from February to May, 2006. The attached spectrograph is either the OMR spectrograph with dispersion of $200\text{\AA}/\text{mm}$ or BFOSC (Beijing Faint Object Spectrograph and Camera) with the grism G4. Both spectrographs give a resolution of $\sim 10\text{\AA}$ and cover the wavelength range from 3800\AA to $\sim 8000\text{\AA}$. The exposure times depend on the apparent magnitudes of these stars from 900 to 3600 seconds. The detail informations of the spectral observations are presented in Table 2. All these spectral data were reduced by the standard procedures with IRAF packages, which include overscan correction for BFOSC only, bias subtraction, flat-field correction. The He/Ne/Ar and Fe/Ar lamps were used for the wavelength calibrations of the OMR and BFOSC spectra. The KPNO standard stars were obtained to perform the flux calibration at each night. All resulting spectra are shown in Figure 2. The spectral classifications are given in Table 2. For those with a poor signal-to-noise spectra (Stars 3, 8, 11), we had to determine their spectral types according their SEDs. All these 11 stars are the main-sequence dwarf stars with the spectral types from M to F, and belong to solar-like stars.

2.5 Reddening

Since all SWIRE regions are at high galactic latitudes, the extinction by the Milky Way extinction A_V of all these stars are no larger than 0.04 from the SDSS "stars" catalog (Adelman-McCarthy et al., 2006) and are therefore neglected in the further analysis. How about the local extinction of these stars? Figure 3 shows the optical color-color diagram for 9 stars. Due to lack of some optical bands, the stars J163948.68+413711.0 and J163754.26+405259.1 are not plotted in this figure. As a comparison, the models of main-sequence stars and giants (Fitzgerald et al., 1970) are also presented as the different curves. All 9 stars are consistent with late type stars as above and are located nearby the curve of the model stars. This indicates that all these stars are slightly obscured. The extinction of K_S is only 10% of A_V and that of $24\mu\text{m}$ is even smaller

3 RESULTS AND ANALYSIS

3.1 IRAC Colors

Figure 4 shows the mid-IR color-color plot for the 11 stars in IRAC bands. The small circles represent the positions of the stars and their corresponding numbers are also labelled. Vega is plotted as a star symbol. There are not any obvious deviation of colors (either $[3.6]-[4.5]$ or $[3.6]-[8.0]$) for Stars 1,4,6,9 from Vega. As Vega has proved to be an IR excess star, for comparison we also plot the position of black-body with Vega temperature of 9600K as plus symbol. Both those stars and Vega show minor excess from black-body in $[8.0]$ band. However, Stars 5,7,8 show large deviation (more than 1 magnitude) in color $[3.6]-[8.0]$. Such a $8\mu\text{m}$ excess can be seen obviously in their SEDs in Figure 6. The remaining Stars 2,3,10,11 show a marginal or modest deviation in $[3.6]-[8.0]$, which show small excess at $8\mu\text{m}$ in SEDs (Figure 6). Only two (Stars 3,7) of these stars show a marginal deviation in $[3.6]-[4.5]$, and the deviations are about 0.2, about 2-3 times typical error. Therefore, we can be sure that most of these $24\mu\text{m}$ excess stars show an excess in the $8\mu\text{m}$ band, and few of them show an obvious excess in the $4.5\mu\text{m}$ band.

3.2 MIPS $24\mu\text{m}$ Excess and Fractional Luminosity

Figure 5 presents the $J-H$ versus $K_S-[24]_{Vega}$ diagram. The dashed are the curve of main sequence stars from Gorlova et al. (2004). All the 11 stars are located at the upper late type stars region. This is consistent with the result of the spectral classification. Almost all of these stars present a large $24\mu\text{m}$ excess. Their $K_S-[24]_{Vega}$ colors are larger than 1, even to 6. These values are far above our selection criterion value of 0.44. Only the late type Star 9 has a $K_S-[24]_{Vega}$ value of 0.51, little larger than 0.44.

Unfortunately, we can not obtain the confirmed far-infrared fluxes for all these stars, because of the low resolution and low sensitivity of the *Spitzer* MIPS $70\mu\text{m}$ and $160\mu\text{m}$ bands. Without the total infrared luminosities of stars, we can not obtain the fractional luminosity f_d , which is defined as the ratio of integrated infrared excess of the disk to bolometric luminosity of star Moór et al. (2006), to characterize the amount of dust. To roughly estimate the fractional dust luminosities, we assumed $F_{IR} \sim \nu F_\nu[24\mu\text{m}]$, as Chen et al. (2005a). The bolometric luminosities of stars are from de Jager & Nieuwenhuijzen (1987). The calculated fractional luminosities are listed in Table 2. The fractional luminosities range from 5×10^{-5} to 3×10^{-3} . It is quite interesting that four of those stars even have the fractional luminosity values higher than 10^{-3} .

3.3 Spectral Energy Distributions

The SEDs of 11 stars are shown in Figure 6. They cover the wavelength range from the optical to the mid-IR bands, including the available photometries of SDSS u,g,r,i,z , 2MASS J,H,K_S , *Spitzer* IRAC four bands and MIPS $24\mu\text{m}$ band. These stars exhibit a variety of mid-IR properties. Five of them show excess only at $24\mu\text{m}$ and four show obviously excess at both $8\mu\text{m}$ and $24\mu\text{m}$. Star 3 even presents excess at shorter wavelength of $3.6\mu\text{m}$. Except Star 9, all the stars show an deviation from the photosphere continuum at mid-IR, indicating the existence of an inner hole of the dust disk (Muzerolle et al., 2006; Young et al.,

3.4 Notes For Individual Source

J160551.07+534841.0, J160650.59+543420.6, J163754.26+405259.1, J163948.68+413711.0, J104205.94+594657.2: These stars have high S/N spectra and a moderate $24\mu\text{m}$ excess (Fig 5) with $K_S-[24]_{Vega}$ between 1 and 4. Their SEDs from the optical to IRAC bands are well consistent with photosphere continuum and only present infrared excess at $24\mu\text{m}$ (Fig 6).

J104508.69+592830.5: This is a M-type star from its spectra (Fig 3). Though it satisfies the $K_S-[24]_{Vega}$ criterion, it presents a marginal excess above the photospheric emission at $24\mu\text{m}$.

J163236.05+405537.3: This is a G-type star and the only source with $8\mu\text{m}$ flux higher than $24\mu\text{m}$ flux in the sample (Fig 3 and Fig 6). Such a feature indicates the peak of infrared emission just between $8\mu\text{m}$ and $24\mu\text{m}$ and the outer radius of the dust disk would be much smaller than 100 au.

J104537.18+570532.9: Though it has a low S/N spectra, combining with its optical and near-infrared colors, we still can classify it as a K-type star. Its SED shows that there is little deviation from photospheric emission at $8\mu\text{m}$. However, it presents a high infrared excess at $24\mu\text{m}$ ($K_S-[24]_{Vega} \sim 5$).

J163611.64+412427.9, J163730.40+403553.1: As above, with the low S/N spectra, J163730.40+403553.1 was classified as a K-type star with the help of either the colors and the SED. J163611.64+412427.9 is a G-type star. Both stars show a high infrared excess at $24\mu\text{m}$. Their SEDs show an abrupt increase from $5.8\mu\text{m}$ to $8\mu\text{m}$ and then continue to increase to $24\mu\text{m}$.

J160122.04+545708.2: For this source, we only have very low signal-to-noise spectra and classified it as a K-type star. With $K_S-[24]_{Vega}$ of 5.62, it is the strongest $24\mu\text{m}$ excess source among the 11 stars. Its SED shows a deviation from photospheric emission even in the near-infrared band, indicating its smaller inner radius of dust disk.

4 DISCUSSION

4.1 The Coincidence Probability

Though we excluded the sources with the fuzzy features, it is still possible that some background and distant galaxies coincide with the position of the candidates and contribute to the measured radiation at $24\mu\text{m}$. Therefore, we need to estimate such a coincidence probability for each source. As Stauffer et al. (2005), we first obtained the cumulative source counts for those with $24\mu\text{m}$ magnitude brighter than the star itself. Here we give an example to explain how we estimated the coincidence probability of the star J160551.07+534841.0. Since it has $24\mu\text{m}$ magnitude of 16.1, we can estimate the cumulative sources counts of 7.8×10^5 per steradian for sources with the $24\mu\text{m}$ magnitude less than 16.1 in the SWIRE ELAIS-N1 fields based on our catalog. This is consistent with that of order of 7×10^5 per steradian for flux density greater than 1.3 mJy (16.1 magnitude in AB system) (Papovich et al., 2004) from the another high galactic latitude field *Spitzer* xFLS. It corresponds to about one source per 54,000 arcsec^2 , considering the previous matched radius of 3 arcsec . The coincidence probability of the background $24\mu\text{m}$ source with magnitude less than 16.1 being close to the line of sight to J160551.07+534841.0 is about 0.0005. Similarly, we estimated the coincidence probabilities of the 11 stars are among 0.0003 and 0.003. Since all the stars locate at the high galactic latitude, it is impossible to be contaminated by cirrus. However, we still can not exclude

4.2 Comparison with Other $24\mu\text{m}$ Excess Samples

Until now, most detected $24\mu\text{m}$ excess stars observed by *Spitzer* are young systems. Low et al. (2005) presented $24\mu\text{m}$ observation for 24 members of the 8-10 Myr old TW Hya association. They found four $24\mu\text{m}$ excess stars. Young et al. (2004) detected several $24\mu\text{m}$ excess stars from young (25 Myr) cluster NGC 2547. Almost all of these stars have $K_S-[24]_{Vega}$ colors less than 2. Only one shows a large $K_S-[24]_{Vega}$ color up to 4. Gorlova et al. (2004) selected $24\mu\text{m}$ excess stars from 100 Myr old open cluster M 47. Seven of the early type stars show smaller excess with $K_S-[24]_{Vega}=0.6-0.9$ and one early type has a color value of 2.4. Three late type stars have $K_S-[24]_{Vega}$ colors between 1 to 4. By studying the 100 Myr Pleiades cluster, Gorlova et al. (2006) obtained an excess fraction of 25% (5/20) for the early-type stars and 10% (4/40) for solar-type stars. All of these stars have $K_S-[24]_{Vega}$ colors less than 1.5. Chen et al. (2005a) obtained the observations of 40 F- and G-type members of the Scorpius-Centaurus OB association with ages between 5 and 20 Myr at $24\mu\text{m}$. They detected 14 objects that possess $24\mu\text{m}$ fluxes $\geq 30\%$ larger than their predicted photosphere. Chen et al. (2005b) obtained the observations of 39 A-through M-type dwarfs with estimated ages between 12 and 600 Myr. Only three stars possess a $24\mu\text{m}$ excess. Su et al. (2006) reported the $24\mu\text{m}$ measurements of 160 A-type main-sequence stars with ages ranging from 5 to 850 Myr. The $24\mu\text{m}$ excess rate is 32%. Beichman et al. (2005) searched for the infrared excess debris disks toward 26 FGK field stars known to have one or more planets. All these stars have a median age of 4 Gyr. None of them show an excesses at $24\mu\text{m}$. Including the Beichman et al. (2005)'s sample, Bryden et al. (2006) extended a well-defined sample of 69 FGK main-sequence field stars also with the median age of 4 Gyr. Only one star shows excess emission at $24\mu\text{m}$. Beichman et al. (2006) searched for the circumstellar dust around a sample of 88 F-M stars, all detected high S/N $24\mu\text{m}$ emission, but only a few present weak $24\mu\text{m}$ excess, though 12 of them present a significant excess $70\mu\text{m}$ emission. Morales et al. (2005) identified two new debris disk candidates with $24\mu\text{m}$ excess at high galactic latitude SWIRE fields. Fajardo-Acosta et al. (2004) also searched for the $24\mu\text{m}$ excess of main-sequence stars in another high latitude xFLS field. Koerner et al. (2010) presented 49 debris disk candidates that were within 25 pc of the Sun and with $V < 9$. The candidate $24\mu\text{m}$ stars we found in the SWIRE fields are the solar-like stars with possible the oldest ages (see the following section). Most of them present large $24\mu\text{m}$ excess with $K_S-[24]_{Vega}$ even approaching 6. Nowadays, only a few main-sequence stars have comparable large $24\mu\text{m}$ excess.

4.3 The Age

Though we have obtained the optical spectra of these $24\mu\text{m}$ excess candidates and classified them based on their spectra and SEDs, we can not determine their ages based on any of the five methods of age estimation for the main-sequence stars (Lachaume et al., 1999). The low resolution of our spectra, and even poor S/N for some faint stars, prevented us to obtain the ages by either the rotation or the iron abundance methods, which need high spectral resolution to measure the rotational velocities or fine absorption lines of different metal elements. The absence of calcium emission and the large uncertainty of the distance determination of

all these stars are the field stars and not born in a molecular clouds, we can not use the kinematics method, too.

So what we can do is to determine their possible location (disk or halo) in our galaxy. As we know now, there are three components except the bulge in our galaxy. They are the thin disk, the thick disk and the halo. The previous works (Bahcall & Soneira, 1984; Gilmore, 1984; Ojha et al., 1999; Chen et al., 2001; Du et al., 2003) showed that the scale height of the thin disk were in the range of 240 to 330 pc and the scale height of the thick disk is in the range of 580 to 1300 pc. Recently, Du et al. (2006) analyzed 21 BATC fields with 15 intermediate-band filters. The scale height they obtained for the thin disk varies from 220 to 320 pc and those for the thick disk varies from 600 to 1100 pc, which is consistent with previous results. Considering that all the three SWIRE fields are at high galactic latitudes of about 40 degree to 50 degree, more than half of the candidate stars have a vertical distance to galactic plane above 600 pc (estimated from their spectral types), which comparable to the scale height of the thick disk. Therefore, these stars could belong to the thick disk or even the halo. The thick disk is an old component with an age around 10 Gyr (Gilmore et al., 1995, 1989). It is quite possible that many of these candidates belong to the population of the very old stars.

4.4 The Fractional Luminosity

There are two major zones of debris in the solar system: the asteroid belt at 2–4 au composed of rocky material that is ground up by collisions to produce most of the zodiacal dust cloud and the Kuiper Belt (KB) that consists of small bodies orbiting beyond Neptune’s orbit at 30 – 50 au (Kim et al., 2005). The excess emission at the mid-IR band *Spitzer* 24 μ m and *IRAS* 25 μ m are sensitive to material at several au (Su et al., 2006). Therefore, the stars with 24 μ m excess are probably those with an planetary systems containing a planetesimal belt corresponding to the asteroidal zone of the solar system (Gorlova et al., 2006). From combination of observation and modelling, Backman & Paresce (1993) and Dermott et al. (2002) determined that the fractional luminosity of our asteroid belt is 10^{-8} to 10^{-7} .

Artymowicz (1996) argued that debris disks are confined to $f_d < 10^{-2}$ and sources with higher fractional luminosity probably contain a significant amount of gas (e.g. T Tau and Herbig Ae/Be stars, ”transition” objects). Zuckerman & Song (2004) hypothesized that the stars with $f_d > 10^{-3}$ are younger than 100 Myr, and therefore a high f_d value can also be used as an age indicator. This is supported by Observations with the *ISO* by Beichman et al. (2005), who suggested a decline in the fraction of stars with the excess IR emission with time, but still with the possibility of existing modest ($f_d > 10^{-5}$) excesses among the older stars (Decin et al., 2000, 2003). Meanwhile, Bryden et al. (2006) selected stars without regard to their age, metallicity, or any previous detection of IR excess. The stars have a median age of ~ 4 Gyr. Their result shows that the debris disks with $f_d \geq 10^{-3}$ are rare around old FGK stars.

On the contrary, Decin et al. (2003) claimed the existence of high f_d disks around older stars. Based on the general evolutionary trend described by Moór et al. (2006), the fractional luminosities of individual systems were found to show a large spread of $10^{-6} < f_d < 10^{-3}$ at almost any age (Decin et al., 2003). Particularly interesting is the relatively high number of older systems ($t > 500$ Myr) with the high values of

Most of our candidates have the values of the fractional luminosity between 10^{-5} to 10^{-4} and four of them even present the high fractional luminosities greater than 10^{-3} . All the four stars have a vertical distance to the disk above 900 pc and have the high possibility to be the old solar-like stars in either the thick disk or in the halo. Therefore, they are possibly the rare systems up to date.

4.5 Physical Explanation and Challenge

How such a large amount of dust still exists in very old solar-like stars? Due to the effect of radiation pressure, Poynting-Robertson drag and collisional destruction, the lifetime of the dust grains are quite short (Beichman et al., 2005; Rieke et al., 2005; Backman & Paresce, 1993; Lagrange et al., 2000; Dominik & Decin, 2003), for example, the dust grain with the smaller size ($\leq 1\mu\text{m}$) has a blown out time less than 100 yrs and the larger dust grain drifted by Poynting-Robertson drag would be destroyed on the timescale of 1-10 Myr (Kim et al., 2005). These are all far shorter than the age of the central stars. Therefore the dust observed must have been recently produced (Beichman et al., 2005). Rieke et al. (2005) pointed out that these reproduced dust in the "debris disk" would arise primarily from collisions between planetesimals and from cometary activity. However, the current model of gas planet formation and isotopic evidence from terrestrial and lunar samples indicate that Jupiter mass planets and Earth-Moon system would formed within several tens millions of years (Silverstone et al., 2006; Kleine et al., 2002, 2003). This still can not explain the high fractional luminosity phenomenon of the old stars. They raise a serious challenge even to the new generation of theoretical models (Moór et al., 2006). The most likely explanation for the presence of debris disk with the high fractional luminosity at ages well above Gyr is delay onset of collisional cascades by late planet formation further away from the star (Dominik & Decin, 2003). However whether such a mechanism can also explain the very old star with an age of 10 Gyr is still questionable.

Besides, the most important is to confirm the ages of these stars with the high fractional luminosity. Therefore the higher S/N and higher resolution spectra are needed in the future observations.

5 SUMMARY

We present 11 debris disk candidates with distance from 300 to 2000pc and age about 10Gyr from *Spitzer* SWIRE fields, with the help of SDSS star catalog and 2MASS point source catalog. They all present $24\mu\text{m}$ excess. The optical spectra obtained from 2.16 telescope at Xinglong, NAOC and SEDs from the optical to mid-infrared are also presented. All these observations shows that:

All of these stars present the late type spectra and the infrared fractional luminosities from 5×10^{-5} to 3×10^{-3} . They would be solar-like stars with the planetary debris disks. Except J104508.69+592830.5, the SEDs of all other stars indicate the existence of an inner hole of the dust disk.

We infer that many of these candidates would have ages of 10 Gyrs, since they are located in the thick disk or in the halo of our galaxy. Therefore, four of these stars could belong to the oldest stars with the high fractional luminosities ($f_d \geq 1 \times 10^{-3}$). Though they are quite rare until now, we indicate that the high fractional luminosity debris disks can exist in the old solar-like star systems.

With the release of *Wide-field Infrared Survey Explorer* (WISE) data, there will be more and more

latitudes will provide us an opportunity to study the properties and evolution of the debris disk evolution in ISM poor environments.

Acknowledgements The authors would like to thank Jia-sheng Huang, Zhong Wang, Jia-rong Shi and Jing-kun Zhao for useful discussion and advice in *Spitzer* data reductions and spectral classification. Also thanks referee's insightful comments. This project is supported by NSFC grants 11173030, 11078017, 10833006, 10978014, 10773014, and partly supported by China Ministry of Science and Technology under State Key Development Program for Basic Research (2007CB815400 and 2012CB821800). S. Wolf was supported by the German Research Foundation (DFG) through the Emmy Noether grant WO 857/2;.

This work was supported by the Key Laboratory of Optical Astronomy, National Astronomical Observatories, Chinese Academy of Sciences. This Also this work, in part, based on observations made with the Spitzer Space Telescope, which is operated by Jet Propulsion Laboratory of the California Institute of Technology under NASA Contract 1407. Funding for the SDSS and SDSS-II has been provided by the Alfred P. Sloan Foundation, the Participating Institutions, the National Science Foundation, the U.S. Department of Energy, the National Aeronautics and Space Administration, the Japanese Monbukagakusho, the Max Planck Society, and the Higher Education Funding Council for England. The SDSS Web Site is <http://www.sdss.org/>. This publication makes use of data products from the Two Micron All Sky Survey, which is a joint project of the University of Massachusetts and the Infrared Processing and Analysis Center/California Institute of Technology, funded by the National Aeronautics and Space Administration and the National Science Foundation.

Facilities: Spitzer, Sloan, 2.16m telescope (NAOC).

References

- Adelman-McCarthy, J. K., et al. 2006, *ApJS*, 162, 38
- Artymowicz, P. 1996, in *The Role of Dust in the Formation of Stars*, ed. H. U. Käüfl & R. Siebenmorgen (New York: Springer), 137
- Aumann, H. H., et al. 1984, *ApJ*, 278, L23
- Backman, D. E., & Paresce, F. 1993, in *Protostars and Planets III*, ed. E. H. Levy & J. I. Lunine (Tucson: Univ. Arizona Press), 1253
- Bahcall, J. N., & Soneira, R. M. 1984, *ApJS*, 55, 67
- Beichman, C. A., et al. 2005, *ApJ*, 622, 1160
- Beichman, C. A., et al. 2006, *ApJ*, 652, 1674
- Benjamin, R. A., et al. 2003, *PASP*, 115, 953
- Bertin, E., & Arnouts, S. 1996, *A&AS*, 117, 393
- Brand, K., et al. 2006, *ApJ*, 641, 140
- Bryden, G., et al. 2006, *ApJ*, 636, 1098
- Bryden, G., et al. 2009, *ApJ*, 705, 1226
- Cao, C., & Wu, H. 2007, *AJ*, 133, 1710
- Chen, A. B., et al. 2001, *AJ*, 121, 309

- Chen, C. H., et al. 2005b, *ApJ*, 634, 1372
- Cutri, R. M., et al. 2003, The IRSA 2MASS All-Sky Point Source Catalog, NASA/IPAC Infrared Science Archive. <http://irsa.ipac.caltech.edu/applications/Gator/>
- Decin, G., Dominik, C., Malfait, K., Mayor, M., & Waelkens, C. 2000, *A&A*, 357, 533
- Decin, G., Dominik, C., Waters, L. B. F. M., & Waelkens, C. 2003, *ApJ*, 598, 636
- de Jager, C., & Nieuwenhuijzen, H. 1987, *A&A*, 177, 217
- Dermott, S. F., Kehoe, T. J. J., Durda, D. D., Grogan, K., & Nesvorný, D. 2002, *ESA SP-500: Asteroids, Comets, and Meteors: ACM 2002*, 319
- Dominik, C., & Decin, G. 2003, *ApJ*, 598, 626
- Du, C., et al. 2003, *A&A*, 407, 541
- Du, C., Ma, J., Wu, Z. Y., & Zhou, X. 2006, *MNRAS*, 372, 1304
- Evans, N. J., II, et al. 2003, *PASP*, 115, 965
- Fadda, D., et al. 2006, *AJ*, 131, 2859
- Fajardo-Acosta, S. B., et al. 2004, *Bulletin of the American Astronomical Society*, 36, 773
- Fazio, G. G. et al., 2004, *ApJS*, 154, 10
- Fitzgerald, M. P., 1970, *A&A*, 4, 234
- Gorlova, N., et al. 2004, *ApJS*, 154, 448
- Gorlova, N., Rieke, G. H., Muzerolle, J., Stauffer, J. R., Siegler, N., Young, E. T., & Stansberry, J. H., 2006, *ApJ*, 649, 1028
- Gilmore, G., 1984, *MNRAS*, 207, 223
- Gilmore, G., Wyse, R. F. G., & Kuijken, K. 1989, *ARA&A*, 27, 555
- Gilmore, G., Wyse, R. F. G., & Jones, J. B. 1995, *AJ*, 109, 1095
- Habing, H. J., et al. 2001, *A&A*, 365, 545
- Hollenbach, D. J., Yorke, H. W., & Johnstone, D. 2000, *Protostars and Planets IV*, 401
- Houck, J. R., et al. 2005, *ApJ*, 622, L105
- Hovhannisyanyan, L. R., et al. 2009, *AJ*, 138, 251
- Huang, J.-S., et al. 2004, *ApJS*, 154, 44
- Jannuzi, B. T., & Dey, A. 1999, in *ASP Conf. Ser. 191, Photometric Redshifts and the Detection of High Redshift Galaxies*, ed. R. J. Weymann et al. (San Francisco, CA:ASP), 111
- Jourdain de Muizon, M., et al. 1999, *A&A*, 350, 875
- Kim, J. S., et al. 2005, *ApJ*, 632, 659
- Kleine, T., Münker, C., Mezger, K., & Palme, H. 2002, *Nature*, 418, 952
- Kleine, T., Mezger, K., & Münker, C. 2003, *Meteoritics & Planetary Science*, vol. 38, Supplement, abstract no.5212, 38, 5212
- Koerner, D. W., Trilling, D. E. et al. 2010, *ApJ*, 710, L26
- Krist, J. E., et al. 2005, *AJ*, 129, 1008
- Lachaume, R., Dominik, C., Lanz, T., & Habing, H. J. 1999, *A&A*, 348, 897
- Lacy, M., et al. 2005, *ApJS*, 161, 41
- Lagrange, A.-M., Backman, D. E., & Artymowicz, P. 2000, *Protostars and Planets IV*, 639

- Lonsdale, C. J., et al. 2003, PASP, 115, 897
- Low, F. J., Smith, P. S., Werner, M., Chen, C., Krause, V., Jura, M., & Hines, D. C. 2005, ApJ, 631, 1170
- McCall, M. L. 2004, AJ, 128, 2144
- Metchev, S. A., Hillenbrand, L. A., & Meyer, M. R. 2004, ApJ, 600, 435
- Meyer, M. R., et al. 2004, ApJS, 154, 422
- Moór, A., Ábrahám, P., Derekas, A., Kiss, C., Kiss, L. L., Apai, D., Grady, C., & Henning, T. 2006, ApJ, 644, 525
- Morales, F. Y., et al. 2005, Bulletin of the American Astronomical Society, 37, 1254
- Muzerolle, J., et al. 2006, ApJ, 643, 1003
- Ojha, D.K., Bienayme, O., Mohan, V., Robin, A.C., 1999, A&A, 351,945
- Oke, J. B., & Gunn, J. E. 1983, ApJ, 266, 713
- Papovich, C., et al. 2004, ApJS, 154, 70
- Rieke, G. H., et al. 2004, ApJS, 154, 25
- Rieke, G. H., et al. 2005, ApJ, 620, 1010
- Schlegel, D. J., et al. 1998, ApJ, 500, 525
- Silverstone, M. D., et al. 2006, ApJ, 639, 1138
- Spangler, C., Sargent, A. I., Silverstone, M. D., Becklin, E. E., & Zuckerman, B. 2001, ApJ, 555, 932
- Stauffer, J. R., et al. 2005, AJ, 130, 1834
- Stoughton, C., et al. 2002, AJ, 123, 485
- Su, K. Y. L., et al. 2005, LPI Contributions, 1280, 143
- Su, K. Y. L., et al. 2006, ApJ, 653, 675
- Surace, J., et al. 2005, SWIRE Data Release 2 Document
- Wen, X. Q., Wu, H., Cao, C., Xia, X. Y., 2007, Research in Astron. Astrophys. (RAA), 7, 187
- Werner, M. W. et al., 2004, ApJS, 154, 1
- Wright, E. L., Eisenhardt, P. R. M., Mainzer, A. K., et al. 2010, AJ, 140, 1868
- Wu, H., Cao, C., Hao, C.-N., Liu, F.-S., Wang, J.-L., Xia, X.-Y., Deng, Z.-G., & Young, C. K.-S. 2005, ApJ, 632, L79
- Wyatt, M. C., & Dent, W. R. F. 2002, MNRAS, 334, 589
- Young, E. T., et al. 2004, ApJS, 154, 428
- Zuckerman, B. 2001, ARA&A, 39, 549
- Zuckerman, B., & Song, I. 2004, ARA&A, 42, 685

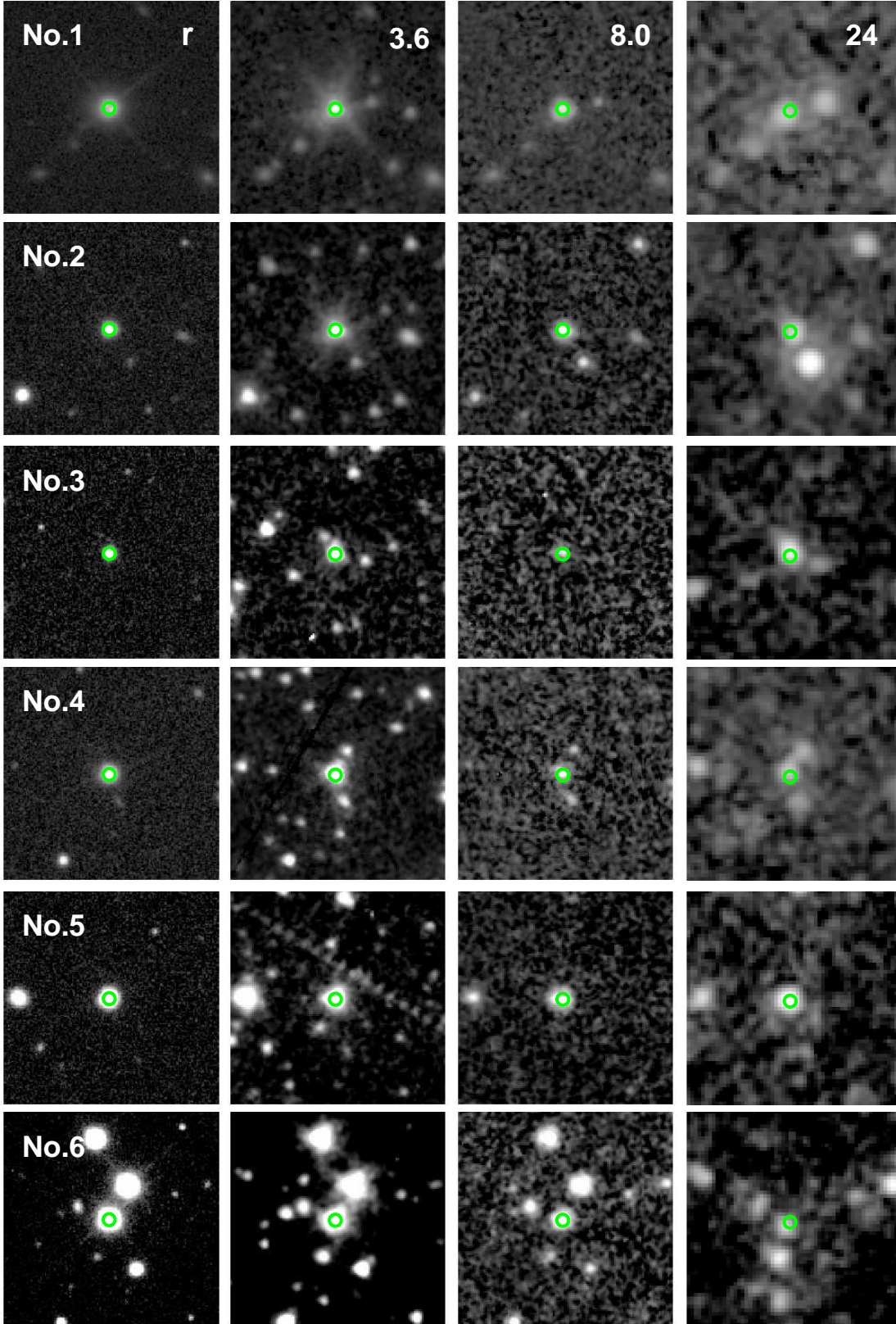


Fig.1 The SDSS r -band, Spitzer 3.6, 8.0 and 24 μm bands images of the 24 μm excess stars. The circle in each image gives the position of stars in r -band with a radius of 1.5".

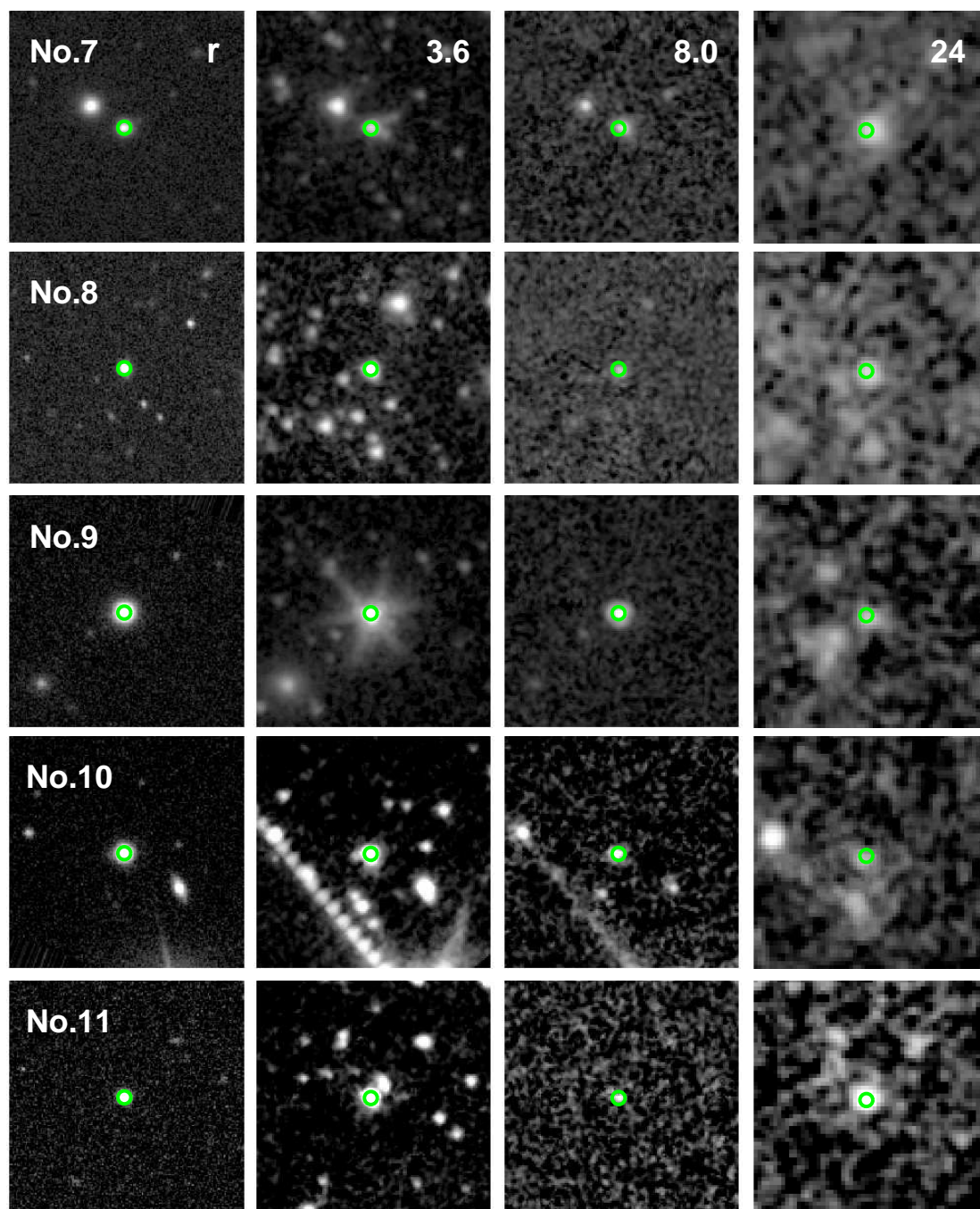


Fig.1 Continued.

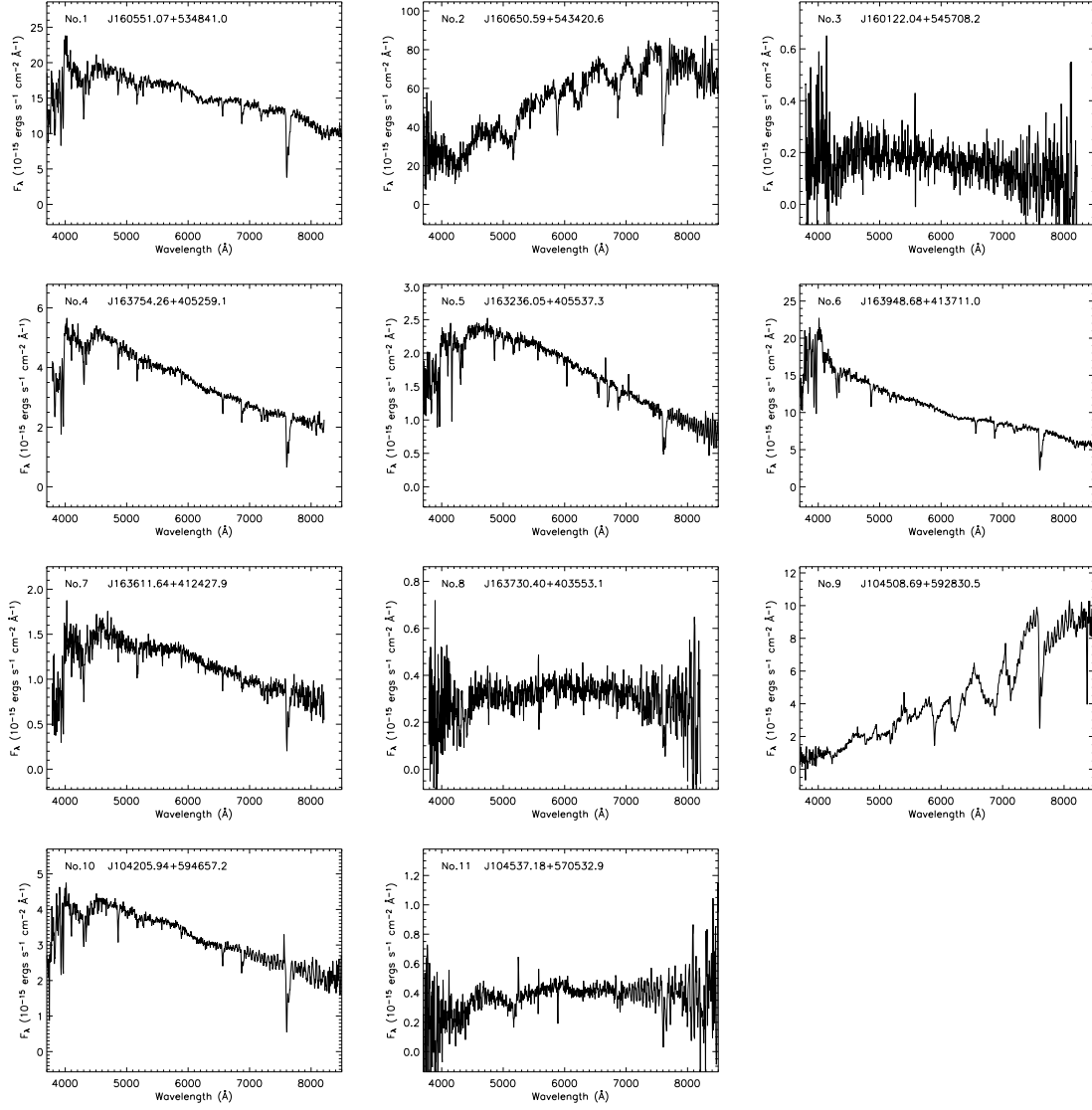


Fig. 2 The observed low resolution optical spectra of the 24μm excess stars. Star 3, 8 and 11 have very low S/N. All the stars present the late type star features.

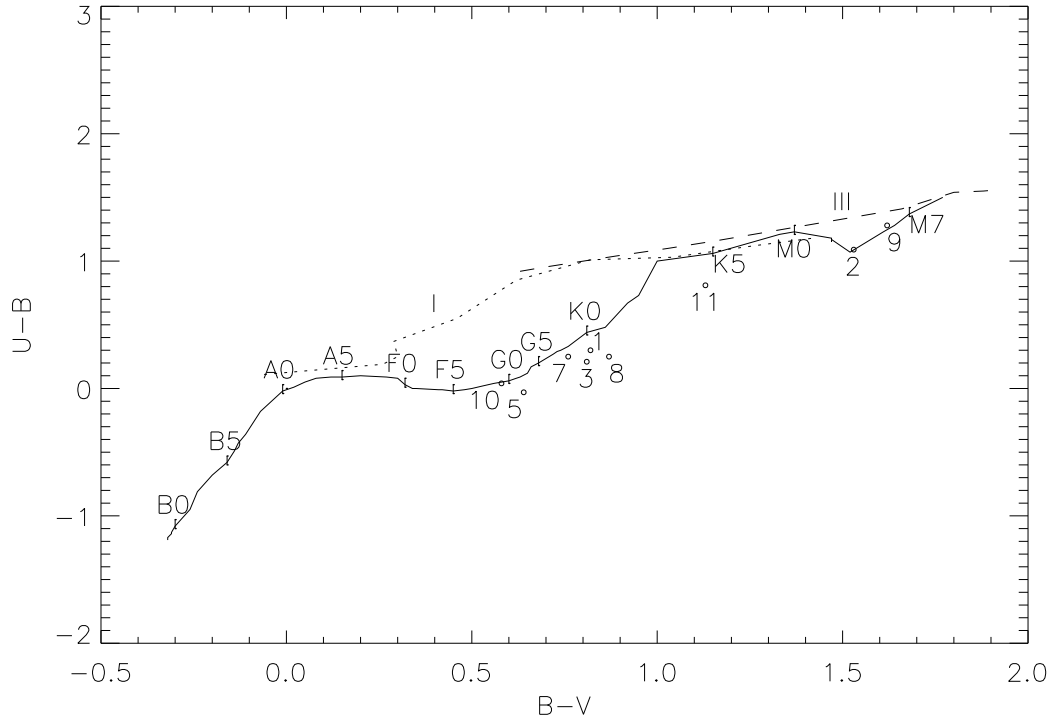


Fig. 3 The optical B-V versus U-B diagram of the $24\mu\text{m}$ excess stars. Each star is symbolized as small circle and labelled with the number. Stars 4 and 6 are lack, because of problems in some optical bands. The dotted line shows the normal dwarf stars in the color-color plot, and the corresponding spectral types are also labelled.

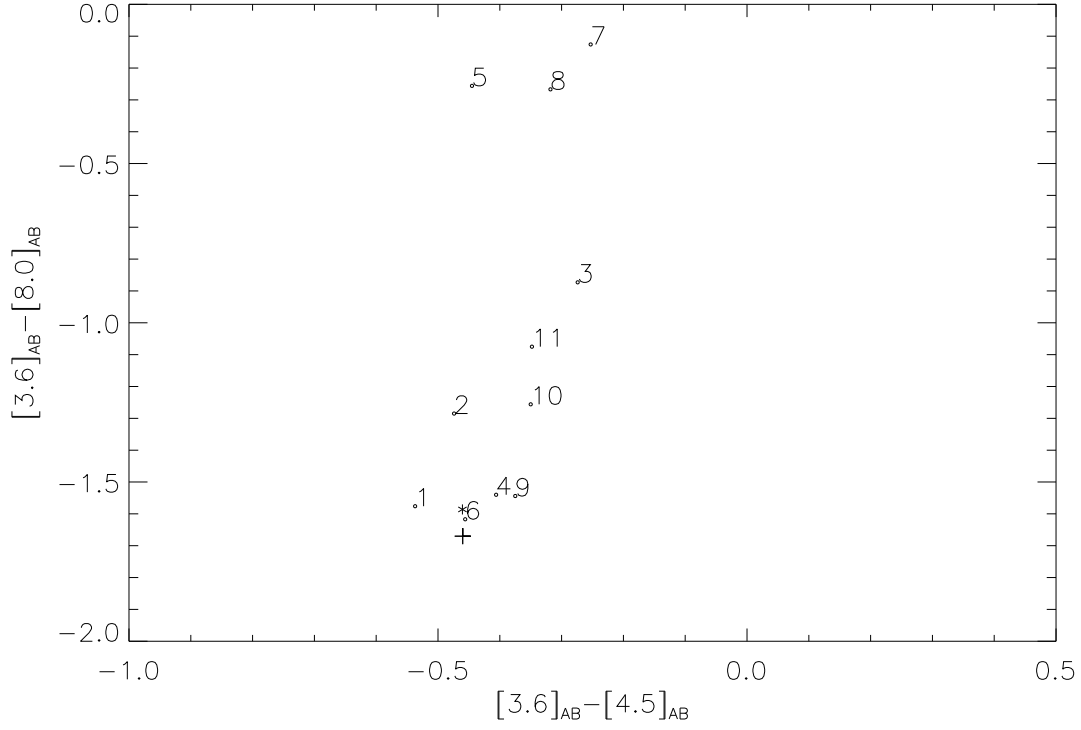


Fig. 4 The mid-infrared IRAC color-color diagram of the $24\mu\text{m}$ excess stars. All the colors are in AB magnitude system. Each star is symbolized as small circle and labelled with the number. The star and plus symbols present the positions of Vega and black-body with temperature of 9600K. Three stars present a high mid-infrared excess at $8\mu\text{m}$ band. Four present a modest excess and the other four show a minor excess at $8\mu\text{m}$ band.

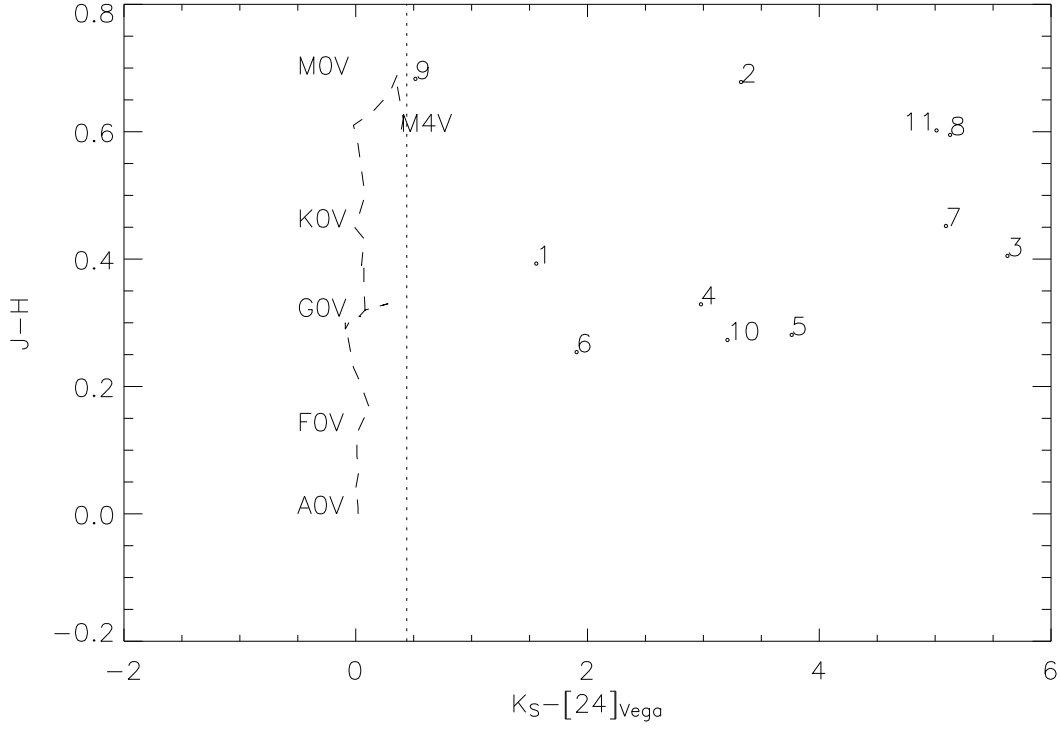


Fig. 5 The plot of $J-H$ versus $K_S-[24]_{Vega}$. All the color are in the Vega magnitude system. Each star is symbolized as small circle and labelled with the number. The dashed curve shows the normal dwarf stars labelled with the corresponding spectral types. The dotted line gives our criteria to select the $24\mu\text{m}$ excess source. Except Star 9, all the stars have $K_S-[24]_{Vega}$ higher than 1 magnitude and four stars present very strong $24\mu\text{m}$ excess.

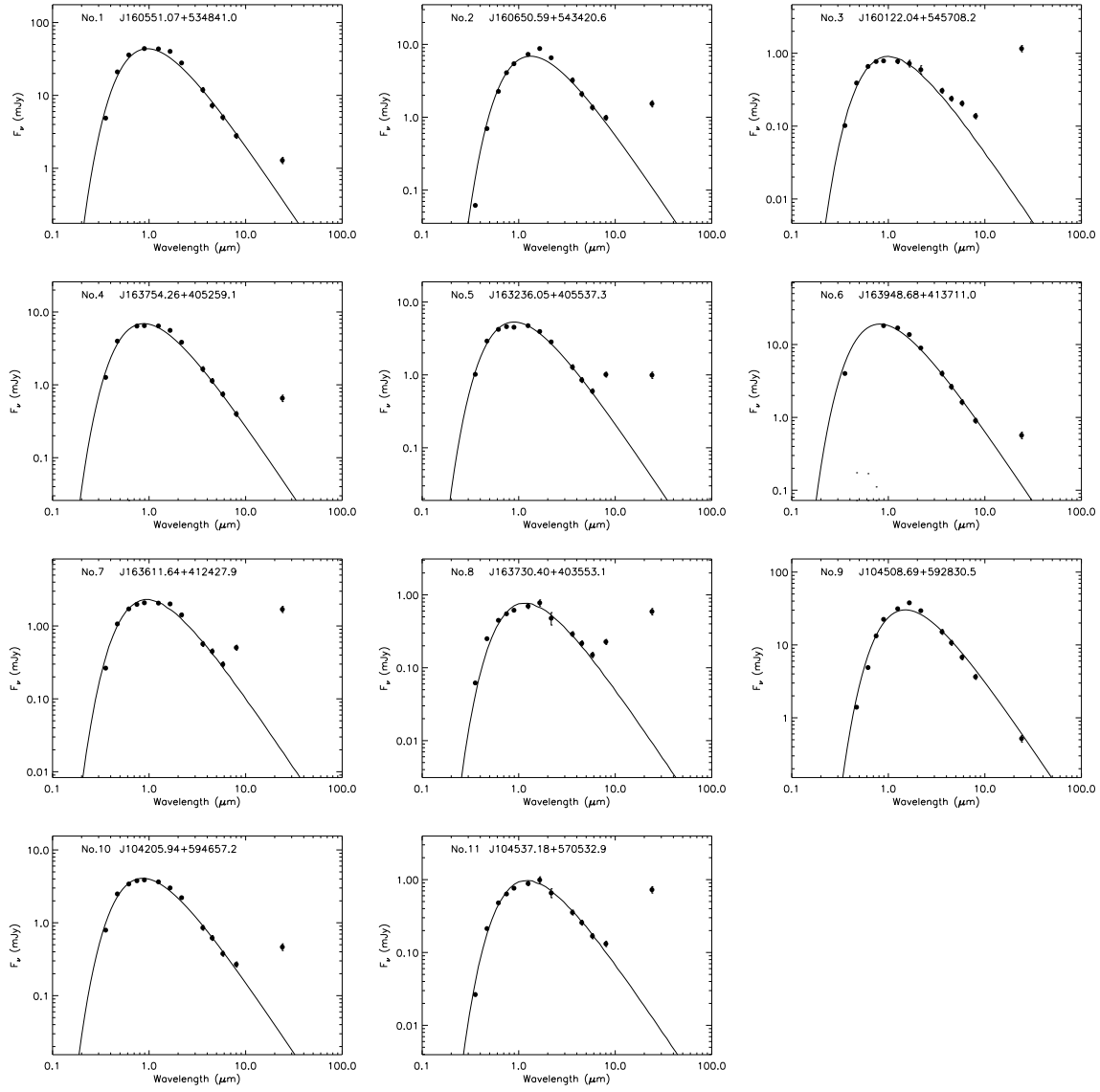


Fig. 6 The optical to mid-infrared SEDs of the 24μm excess stars. The black points give the fluxes of the SDSS five bands (u, g, r, i, z), the 2MASS three bands (J, H, K_S) and the *Spitzer* IRAC four bands and MIPS 24μm band. The photospheric emission is plotted as solid curves. Comparing with the solid curves, all these stars present excess at mid-infrared.

Table 1 The names, magnitudes and colors of the 11 $24\mu\text{m}$ excess stars.

NO.	Name	u	g	r	i	z	J	H	K_S	$[3.6]_{AB}$	$[4.5]_{AB}$	$[5.8]_{AB}$	$[8.0]_{AB}$	$[24]_{AB}$	$K_S-[24]_{Vega}$
1	J160551.07+534841.0	14.64	13.13	12.52	13.38	12.29	11.41	11.02	10.95	13.71	14.25	14.65	15.29	16.13	1.56
		± 0.02	± 0.00	± 0.00	± 0.00	± 0.01	± 0.02	± 0.02	± 0.02	± 0.08	± 0.08	± 0.08	± 0.08	± 0.10	± 0.10
2	J160650.59+543420.6	19.39	16.83	15.52	14.88	14.56	13.35	12.67	12.52	15.13	15.61	16.07	16.42	15.94	3.32
		± 0.04	± 0.02	± 0.02	± 0.02	± 0.02	± 0.03	± 0.02	± 0.02	± 0.08	± 0.08	± 0.08	± 0.08	± 0.10	± 0.10
3	J160122.04+545708.2	18.84	17.46	16.86	16.69	16.66	15.78	15.38	15.12	17.68	17.96	18.12	18.56	16.24	5.62
		± 0.03	± 0.03	± 0.02	± 0.02	± 0.02	± 0.07	± 0.11	± 0.13	± 0.08	± 0.08	± 0.08	± 0.09	± 0.10	± 0.17
4	J163754.26+405259.1	16.10	14.94	-	14.39	14.37	13.49	13.16	13.10	15.86	16.26	16.72	17.40	16.86	2.98
		± 0.02	± 0.01	± 0.00	± 0.01	± 0.02	± 0.02	± 0.03	± 0.03	± 0.08	± 0.08	± 0.08	± 0.08	± 0.10	± 0.11
5	J163236.05+405537.3	16.34	15.28	14.85	14.76	14.77	13.82	13.54	13.43	16.13	16.58	16.96	16.39	16.41	3.76
		± 0.02	± 0.01	± 0.01	± 0.02	± 0.02	± 0.03	± 0.05	± 0.05	± 0.08	± 0.08	± 0.08	± 0.08	± 0.10	± 0.11
6	J163948.68+413711.0	14.85	-	-	-	13.25	12.44	12.19	12.18	14.90	15.35	15.88	16.51	17.01	1.91
		± 0.01	± 0.05	± 0.03	± 0.03	± 0.01	± 0.02	± 0.02	± 0.02	± 0.08	± 0.08	± 0.08	± 0.08	± 0.10	± 0.11
7	J163611.64+412427.9	17.81	16.37	15.82	15.67	15.60	14.73	14.27	14.18	17.02	17.27	17.72	17.14	15.83	5.09
		± 0.02	± 0.02	± 0.01	± 0.02	± 0.02	± 0.03	± 0.05	± 0.06	± 0.08	± 0.08	± 0.08	± 0.08	± 0.10	± 0.12
8	J163730.40+403553.1	19.38	17.94	17.28	17.06	16.93	15.90	15.30	15.36	17.74	18.06	18.46	18.01	16.97	5.13
		± 0.03	± 0.01	± 0.01	± 0.01	± 0.02	± 0.08	± 0.10	± 0.19	± 0.08	± 0.08	± 0.09	± 0.08	± 0.10	± 0.22
9	J104508.69+592830.5	18.88	16.08	14.69	13.60	13.02	11.77	11.09	10.89	13.45	13.83	14.32	14.99	17.11	0.51
		± 0.05	± 0.01	± 0.02	± 0.02	± 0.01	± 0.03	± 0.03	± 0.02	± 0.08	± 0.08	± 0.08	± 0.08	± 0.11	± 0.11
10	J104205.94+594657.2	16.61	15.45	15.08	14.97	14.93	14.11	13.83	13.70	16.57	16.92	17.46	17.83	17.23	3.21
		± 0.01	± 0.03	± 0.02	± 0.01	± 0.02	± 0.03	± 0.04	± 0.04	± 0.08	± 0.08	± 0.08	± 0.08	± 0.11	± 0.12
11	J104537.18+570532.9	20.30	18.12	17.21	16.90	16.69	15.64	15.04	15.02	17.53	17.88	18.34	18.60	16.75	5.01
		± 0.05	± 0.02	± 0.02	± 0.02	± 0.02	± 0.07	± 0.11	± 0.14	± 0.08	± 0.08	± 0.09	± 0.09	± 0.10	± 0.18

Table 2 The log of observation, spectral type and the fractional luminosity of the 11 $24\mu\text{m}$ excess stars.

NO.	Name	Date of Obs.	Exptime sec	Instrument	Slit arcsec	Sp.	f_d
1	J160551.07+534841.0	Feb. 4, 2006	900	OMR 200Å/mm	2.5	G8V	7.0e-5
2	J160650.59+543420.6	Apr. 28, 2006	2400	BFOSC Grism#4	1.8	M0V	7.4e-4
3	J160122.04+545708.2	May. 6, 2006	3600	OMR 200Å/mm	2.0	K0V	3.2e-3
4	J163754.26+405259.1	May. 5, 2006	2700	OMR 200Å/mm	2.0	G2V	2.1e-4
5	J163236.05+405537.3	Feb. 21, 2006	3600	BFOSC Grism#4	1.1	G3V	4.2e-4
6	J163948.68+413711.0	Feb. 4, 2006	1800	OMR 200Å/mm	2.5	F8V	5.4e-5
7	J163611.64+412427.9	May. 5, 2006	2700	OMR 200Å/mm	2.0	G7V	1.8e-3
8	J163730.40+403553.1	May. 6, 2006	3600	OMR 200Å/mm	2.0	K4V	2.1e-3
9	J104508.69+592830.5	Feb. 3, 2006	2400	OMR 200Å/mm	2.5	M3V	6.9e-5
10	J104205.94+594657.2	Feb. 3, 2006	2400	OMR 200Å/mm	2.5	G0V	2.4e-4
11	J104537.18+570532.9	Feb. 3, 2006	3600	OMR 200Å/mm	2.5	K6V	2.3e-3